APCC
APEC CLIMATE CENTER

RESEARCH REPORT

APCC
APEC CLIMATE CENTER

PREFACE

It is our pleasure to present this report on the APEC Climate Center (APCC)'s research activities in 2013, which has been a very productive year for our Center.

APCC has expanded its research scope, in response to regional societal and scientific needs. While building expertise in climate prediction remains a priority, we are extending our reach to include policy-relevant climate applications and value-added climate information products.

APCC has accelerated efforts to better our service to the region. As one of the main services provided by APCC, the MME 3-month prediction information has been productively applied by scientists in developing countries that are unable to produce their own prediction information. Furthermore, in order to better prepare for climate-related hazards in a timely manner, APCC launched its 6-month MME prediction service in September 2013. We also began to release forecasts of the Boreal Summer Intraseasonal Oscillation (BSISO), starting from July 2013, as the world's first operational BSISO forecast service. Our researchers also achieved great success in publishing their papers in noted academic journals. Dr. Ok-Yeon Kim, for example, published a paper in *Climate Dynamics* and her research was later selected as one of the Research Highlights by another distinguished journal, *Nature Climate Change*. The following research report provides more information about our research outcomes from 2013.

We will continue to promote the best use of our research outcomes in various scientific and application areas. Our successes and achievements would not have been possible without the support of our valued partners. In this regard, I extend my thanks to you and I hope you enjoy this 2013 Research Report.

Chin-Seung Chung
Director, APEC Climate Center

CONTENTS

Revising the DSSAT/CERES-Rice Model to Simulate the Impacts of Climate Change on Rice Yield in Asia

■■ **Dr. Qingguo Wang** | Climate Change Research Team

APCC

RESEARCH REPORT 2013-07

Revising the DSSAT/CERES-Rice Model to Simulate the Impacts of Climate Change on Rice Yield in Asia

Dr. Qingguo Wang | Climate Change Research Team

ABSTRACT

The CERES-Rice model has been used to simulate rice plant responses to CO_2 enrichment and climate change and to explore adaptation options. However, it was developed decades ago, contains many empirical equations, and the model parameters have little plant physiological meaning and have to be determined under specific conditions. Further, it does not incorporate recent knowledge about how crops respond to changing climates and management practices. For example, it uses an empirical Radiation Use Efficiency approach to calculate plant growth. There are evidences that these empirical equations could result in a wrong direction of interactions among involved factors. This study improved on the original model by using biochemical photosynthetic equations to develop a new approach. The revised model had better agreement than the original version between simulations and observations of rice growth and yield of three cultivars collected from four experiments with treatments of N applications combined with irrigations conducted in Thailand and the Philippines. The simulated rice yield showed increases or decreases in 2020, 2050, and 2090 depending on the climate scenarios and treatments. This study illustrated the potential for the revised model to improve rice yield gap analyses to find a solution that improves farmers' yields, such as changing transplanting dates under different environmental conditions. However, further evaluation of the revised model is needed under changing climate conditions, such as with data from FACE experiments. The revised CERES-Rice model performs better than the original and can be used for forecasting rice yield and determining optimal management practices.

1. INTRODUCTION

Rice (Oryza sativa L.) is the most important food crop globally; feeding more than half of the world's population. East, South, and Southeast Asia produce and consume 90% of the global rice crop (Fig. 1). Demand for rice would continue to grow as a result of growing population (Cho and Oki 2012). The production of rice in Asia has increased markedly with the introduction and widespread adoption of modern crop production technologies. However, rice yields are stagnant or declining and there are large gaps between the climatically and genotypically determined potential and actual yields. The ability to sustain yields is likely threatened by climate change, impending water scarcity, soil degradation, and the pollution of ground and surface water.

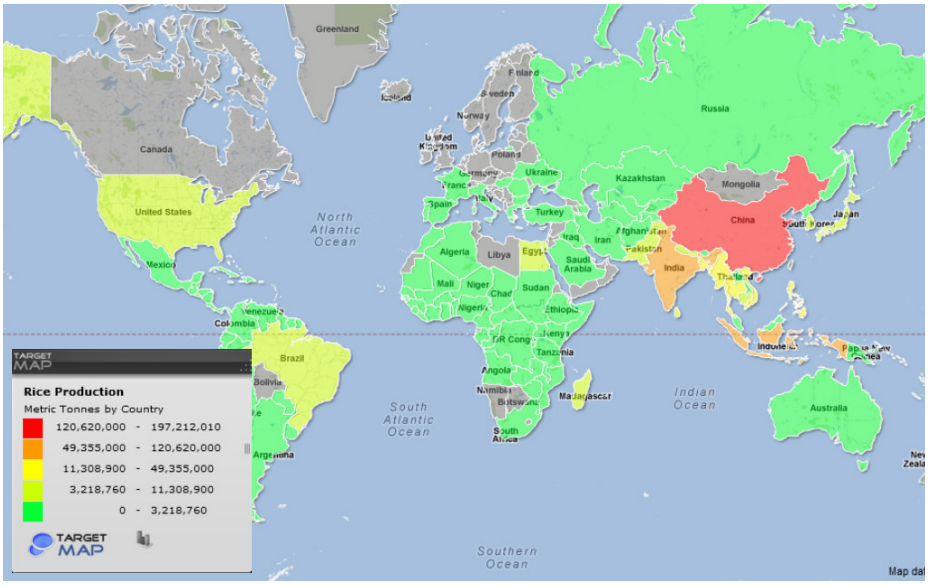

Figure 1 World rice production map

Continuing global changes (Yang et al. 2013) could positively or negatively impact aspects of our current lives, such as human health, environment, and agriculture. In an agricultural system, crop production depends on an integrated response to climate change, new cultivars, and management techniques. In general, yield declines have been reported in response to CO_2 enrichment and higher temperatures (Cho and Oki 2012). Elevated CO_2 could increase plant body temperatures by reducing transpiration, further enhancing the effects of higher air temperatures. Lobell et al. (2011) showed that in many countries since 1980 climate trends were large enough to offset a significant proportion of the potential increases in average crop yields due to technological advances, CO_2 fertilization, and other factors. By 2100, potentially, atmospheric CO_2 will rise to 936 mmol mol^{-1}; temperatures will rise by 4.8 °C in the RCP8.5 scenario (Meiinshause et al. 2011); precipitation will become more variable; and extreme weather patterns will become more frequent, intense, and last longer (IPCC 2007). It is thus imperative to continue to advance fundamental knowledge of crop responses to climate change, reduce uncertainties in impact projections, and assess future risks (IPCC 2007). Stakeholders have increasing demands concerning adaptation strategies that improve the resilience of crop systems to stresses induced

by climate change (Howden et al. 2007). Adaptation requires detailed understanding of the likely impacts of climate change in small agricultural regions, which further increases the need for crop modeling.

Crop models provide a means to quantify the effects of climate, weather conditions, soil, management, and genotypes and their interactions on crop growth, development, yield, resource use efficiency, and environmental impacts. Process-based crop models have been increasingly used in agricultural and environmental studies for several decades to quantify the gaps between potential and actual yields, to evaluation management options, and to determine likely environmental impacts. The models can provide a unique means of quantifying the potential impacts of climate change on crop performance and water use requirements and in the evaluation of adaptation strategies. For example, Matthews et al. (1995) simulated the response of rice yields to climate change using the ORYZA model, Fleisher et al. (2010) reported potato gas exchange rates using the SPUDSIM model, and Salam et al. (2010) studied rice management using the CERES-Rice model. Chen et al. (2010) simulated climate and water management for a winter wheat and summer corn rotation using the APSIM model. Liu et al. (2011) used the DSSAT model to estimate water content, crop yields, and nitrate-N loss.

A number of rice growth models have been developed in the past few decades and used for yield prediction. These models can be divided into two groups. One group is the process-based crop models, such as DSSAT/CERES-Rice (Jones et al. 2003) and ORYZA2000 (Bouman et al. 2001). These models were originally developed for rice yields under uniform conditions, i.e., at the plot scale. To predict yields at a larger scale, an appropriate aggregation method must be applied. Another group of models is the empirical or semi-empirical models, which can be directly applied at a large scale with low input data, such as SIMRIW (Horie et al. 1995) and GLAM (Challinor et al. 2004). However, this group may not be appropriate to apply to a complex terrain with spatial variation in soils, climate, and management practices. The model with low input data cannot capture some important biophysical processes that are essential for evaluating the response of plants to the environment and management practices. Table 1 shows 13 rice models evaluated by the Rice Team

of the Agricultural Model Intercomparison and Improvement Project (Rosenzweig et al. 2013). These are the most commonly used rice models and are mostly processed-based.

Table 1 The rice models evaluated by the Agricultural Model Intercomparison and Improvement Project (AgMIP) Rice Team

	Model name	Affiliation of participating scientist	Country
1	APSIM-ORYZA	CSIRO Ecosystem Sciences	Australia
2	CERES-Rice	International Fertilizer Development Institute APEC Climate Center	USA S. Korea
3	DNDC-Rice	National Institute for Agro-Environmental Sciences	Japan
4	GECROS	Wageningen University	Netherlands
5	GEMRICE	National Agriculture and Food Research Organization	Japan
6	McWLA	Chinese Academy of Sciences	China
7	NIAES	National Institute for Agro-Environmental Sciences	Japan
8	ORYZA2000	International Rice Research Institute	
9	RiceGrowth	Nanjing Agricultural University	China
10	SAMARA	CIRAD, UMR AGAP	France
11	SIMRIW	National Institute for Agro-Environmental Sciences	Japan
12	STICS	Institute National de Recherce Agronomique	France
13	WARM	University of Milan	Italy

The DSSAT/CERES-Rice model, included in the decision support system for agrotechnology transfer (DSSAT) developed by the International Benchmark Systems Network for Agrotechnology Transfer, is a widely used decision support system (Jones et al. 2003; Timsina and Humphreys 2006). A considerable number of studies based on CERES-Rice models have been conducted in Asian regions, in Australia (Timsina and Humphreys 2006), China (Jing and Jin 2009), India (Sarkar and Kar 2008), and South Korea (Yun 2003; Kim et al. 2002; Lee et al. 2012). The model assumes that rice cultivars, weather, soils, and crop management are the primary influences on rice productivity. Rice growth and development can interact with atmospheric and soil conditions. However, the potential net growth rate is calculated by converting daily canopy-intercepted radiation into plant dry matter using an empirical, rice-specific radiation use efficiency parameter.

Evidence shows that a multiplicative model can result in a wrong direction of interaction among involved factors. This type of model error can lead to unreliable predications of the impact of climate change on crop yields. The crop photosynthesis model cannot capture well the effects of CO_2 enrichment on plant growth in a physiological way, and often has large uncertainty. As pointed out by Rotter et al. (2011), the model does not incorporate the latest knowledge of responses of rice systems to potential climate change and elevated CO_2 and management practices. One possible reason is that the model was originally developed under ambient CO_2 conditions; however, when used to assess the effects of elevated CO_2 under climate change conditions, only some parameters were modified from elevated-CO_2 experiments (e.g., Equations (2) and (3)). The model for estimating the effects of climate change needs to capture the responses of crop growth and development to all major environmental variables, especially the interaction of CO_2 with other climatic factors. However, studies dedicated towards improving the CERES-Rice model for climate impact assessment are rare.

In this study, we attempted to make substantial modifications to CERES-Rice to develop an hourly photosynthesis model based on the biochemical FvCB model (Farquhar et al. 1980), which can predict the effect of CO_2 enrichment and climate change on rice yield. The revised model was then tested against observations at several rice field experiments in Asia.

2. THE CERES-RICE MODEL REVISIONS

The CERES-Rice model is a physiological-based rice (*Oryza sativa* L.) model (the latest version is 4.5) a crop model contained in the Decision Support System for Agro-technology Transfer (DSSAT) developed by the International Benchmark Systems Network for Agrotechnology Transfer (IBSNAT). The model can simulate rice crop growth, development, and yield potential on a uniform area of land by combining the properties of rice genetics, soil, weather, and management. The step for input

data is daily and the minimum data requirements for the operation, calibration, and validation of the model are provided by Hunt and Boote (1994). The CERES-Rice model processes have been incompletely documented in a fragmented way in various publications (Singh et al. 1993; Singh et al. 2002). Since the focus of this report is on revision of the growth part of the model, only the growth features of model components are outlined in Figure 2 and described here. The potential net photosynthetic rate (PCARB) is estimated by (the Fortran code) :

PCARB=RUEA*PAR*RUEX/EPLANTS*(1.0-AMIN1(Y1,Y2)) (1)

where PCARB is potential dry matter production, PAR is photosynthetically active solar radiation, RUEX is the conversion factor of PAR to dry matter, and AMIN1 is the minimum function.

When it includes the impact of CO_2 and other environmental stresses, it is expressed as (the Fortran code):

CARBO=PCARB*PCO2*AMIN1(PRFT,SWFAC,NSTRES,TSHOCK,PStres1,KSTRES) (2)

where CARBO is the net photosynthesis rate, PCO2 is the impact of CO_2 concentration, and the parameters in parentheses are environmental factors. The impact of CO_2 concentration is calculated as (the Fortran code):

PCO2 = TABEX (CO2Y,CO2X,CO2,10) (3)

where TABEX is the table lookup function, and the values are obtained from (the Fortran code)

DATA CO2X1/ 0, 220, 330, 440, 550, 660, 770, 880, 990, 9999/

DATA CO2Y1/0.00, 0.71,1.00, 1.08,1.17,1.25,1.32,1.38, 1.43, 1.50/

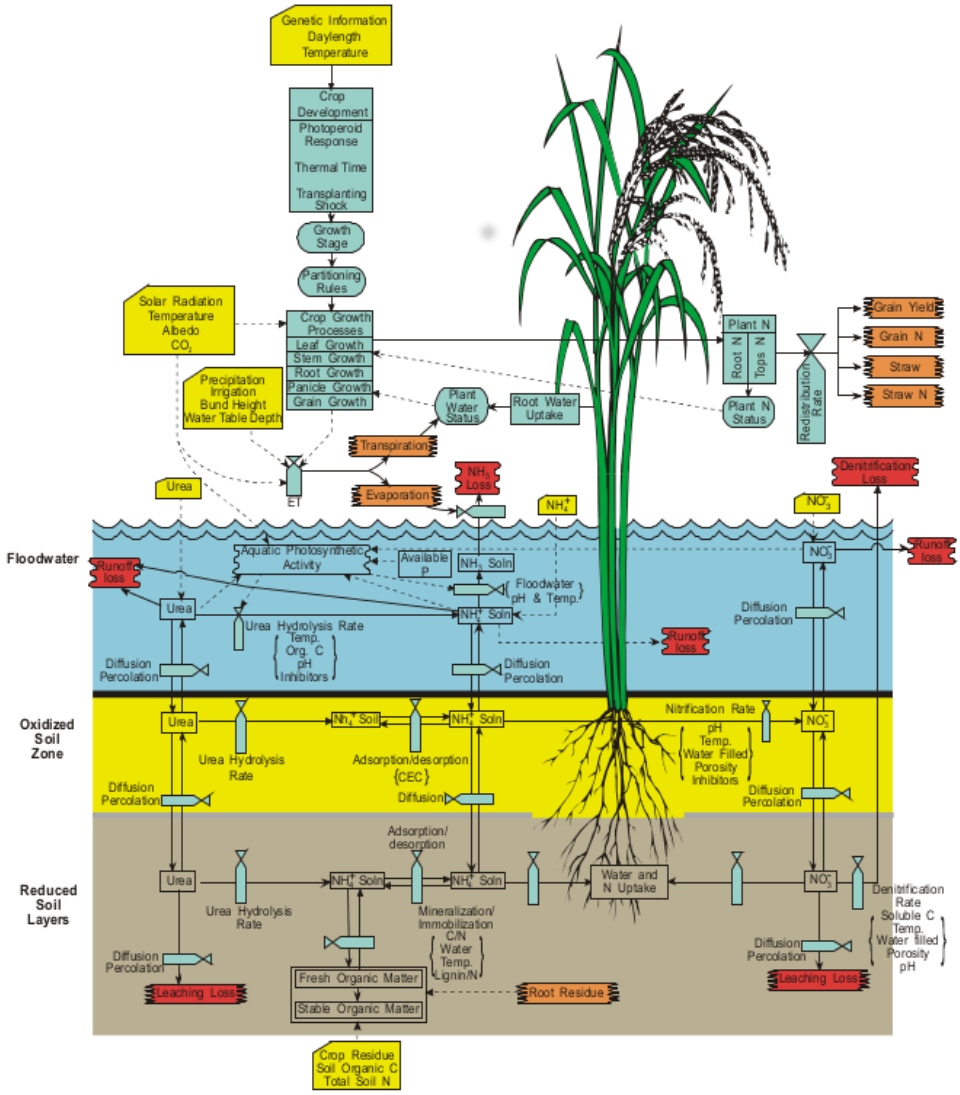

Figure 2 Schematic diagram of the original CERES-Rice model (adopted from Singh et al. 2002)

The original version of CERES Rice (V 4.5) was modified as described in Figure 3. The net photosynthetic rate of a canopy element depends, *inter alia*, on the amount of ribulose-1,5-bisphosphate carboxylase/oxygenase (Rubisco), the capacity for RuBP regeneration, the rate of inorganic phosphate supply to the chloroplast for photosynthesis of that element, its absorbed irradiance, its CO_2 concentration at the sites of carboxylation,

and its temperature. Considering the heterogeneous radiation in canopies and the non-linear response of photosynthesis to irradiance and CO_2, following de Pury and Farquhar (1997) and Wang and Leuning (1998), canopy photosynthesis is estimated by integrating the photosynthesis from sunlit and shaded leaves.

2.1 Fraction of sunlit and shaded leaves

The fractional area of sunlit leaves over a canopy decreases exponentially with the cumulative leaf area index from the canopy top. The fractions of sunlit and shaded leaves, f_{sun} and f_{sh}, respectively, are calculated from:

$$f_{sun} = \exp(-k_b L) \quad (4)$$

$$f_{sh} = 1 - f_{sun} \quad (5)$$

where k_b is the direct beam extinction coefficient of the rice canopy.

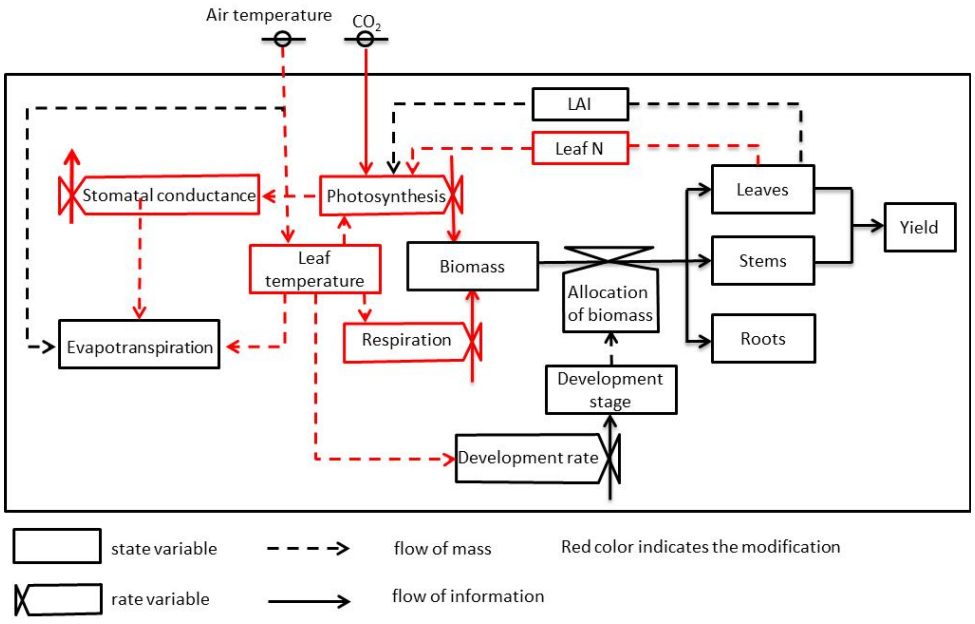

Figure 3 Outline of the model revisions: growth, development, and yield

2.2 Radiation absorption

Radiation attenuation through canopies can be described by Beer's law (Monsi and Saeki 1953; Goudriaan 1977). It is now generally accepted that the solar radiation flux density absorbed by the sunlit leaves in the canopy is given as the sum of the components of direct-beam, I_b; scattered direct-beam, I_s; and diffuse radiation, I_d, and shaded leaves receive diffuse light and scattered direct beam radiation. The radiation received by shaded leaves is given by:

$$I_{sh} = I_d + I_s \quad (6)$$

The radiation absorbed by sunlit leaves is calculated by:

$$I_{sun} = I_{sh} + I_{bsun} \quad (7)$$

where $I_{b\mathrm{sun}}$ is the beam radiation absorbed by sunlit leaves.

2.3 Calculation of day-length and hourly weather data

Solar day length and time of sunset and, time of sunrise are calculated by Subroutine DAYLEN. Hourly PAR and hourly temperature are calculated by Subroutine HMET. The hourly radiation, Radhr, is calculated by:

$$\mathrm{Radhr} = \mathrm{SINB(1.0+0.4SINB)SRAD*1.0E6/ISINB} \quad (8)$$

where SRAD is daily solar radiation. The hourly air temperature, Tairhr, is estimated by:

$$\mathrm{Tairhr} = \mathrm{T_{MIN}} + (\mathrm{T_{MAX}} - \mathrm{T_{MIN}})*\mathrm{SIN(T)} \quad (9)$$

where T_{MIN} and T_{MAX} are the minimum and maximum temperature, respectively.

2.4 Leaf photosynthesis

Potential rice leaf gross photosynthesis, the net photosynthesis in the absence

of water stress, can be estimated by the biochemical equation of CO_2 assimilation originally developed by Farquhar et al. (1980) for C_3 leaves, and later modified by Sharkey (1985), Harley et al. (1992a, b) and Wullschleger (1993):

$$A_p = 44 \times 10^{-6} min\{W_c, W_j, W_p\}\left(1 - \frac{\Gamma^*}{C_C}\right) \quad (10)$$

with

$$W_c = V_{c\max}\frac{C_c}{C_c + \mathrm{K_c}(1 + \frac{\mathrm{O}}{\mathrm{K_o}})} \quad (11)$$

$$W_j = J\frac{C_c}{4C_c + 8\Gamma^*} \quad (12)$$

$$W_p = 3T_p\frac{C_c}{C_c - \Gamma^*} \quad \text{for } C_c > \Gamma^* \quad (13)$$

where the constant 44 × 10^{-6} is the converter to g CO_2 m^{-2} leaf s^{-1}, W is the carboxylation rate, and subscripts *c*, *j*, and *p* indicated the state limited by Rubisco (A_c state), the RuBP regeneration (A_j state), and TPU (T_p state), respectively; min{} denotes 'the minimum of'; $V_{c\max}$ is the maximum rate of carboxylation; $V_{o\max}$ is the maximum rate of oxygenation; C_c and O are the partial pressures of CO_2 and O_2 at Rubisco; K_c and K_o are the Michaelis-Menten constants for carboxylation and oxygenation, respectively; O is the oxygen concentration; J is the potential rate of electron transport that is dependent upon incident light irradiance; the factor 4 in equation 3 indicates that the transport of four electrons will produce sufficient ATP and NADPH for the regeneration of RuBP in the Calvin cycle; Γ^* is the C_c-based CO_2 compensation point in the absence of mitochondrial respiration in the light; and T_p is the rate of phosphate release in triose phosphate utilization (starch and sucrose production). Provided that the resistance for CO_2 from intercellular spaces to mesophyll cells is negligible, C_c can be estimated by:

$$C_c \approx C_i = 0.7C_a + 0.3\Gamma^* \quad (14)$$

where C_i is the partial pressures of CO_2 in the intercellular air space, and the ratio

0.7 is the rate of change of C_i with respect to C_a, which has held over a wide range of environmental conditions for many C_3 species (Morison, 1987; Boote and Pickering, 1994).

In Eq. (12), the potential electron transport rate (J) is related to the light-saturated rate of electron transport, J_{max}, through empirical relationships such as the following (Farquhar and Wong 1984):

$$J = \frac{\sigma I_a + J_{\max} - \sqrt{(\sigma I_a + J_{\max})^2 - 4\theta I_a J_{\max}}}{2\theta} \quad (15)$$

where I_a is the absorbed light, σ is the electron transport efficiency of PS II on the basis of light absorbed by both photosystem I and II, and θ is a curvature parameter. The variable I_a is calculated as:

$$I_a = \alpha I(1-f)/2 \quad (16)$$

where I is the incident light in photosynthetic flux density (μ mol photons m^{-2} s^{-1}) (PFD), α is leaf absorbance in PAR (0.85), and f is the spectral correction factor (0.2). The denominator 2 is because of the assumption that half of the light absorbed reaches each photosystem.

The CO_2 compensation point in the absence of day respiration (Γ^*) is temperature dependent and calculated as:

$$\Gamma^* = 36.9 + 1.88 \cdot (T_L - 25) + 0.036 \cdot (T_L - 25)^2 \quad (17)$$

where T_L is leaf temperature in °C. An Arrhenius function is used to calculate the temperature dependence of K_c, K_o, R_d, and T_p:

$$parameter = parameter_{25} \exp\{E_a(T_L - 25)/[298R(T_L + 273)]\} \quad (18)$$

where $parameter_{25}$ is the value of a parameter at 25 °C, E_a is the activation energy and R is the universal gas constant (8.31 J K^{-1} mol^{-1}). The temperature responses of parameters V_{cmax} and J_{max} are expressed by a modified Arrhenius function (Medlyn et al. 2002) as:

$$paremeter = paremeter_{\max 25} \exp\left[\frac{(T_L - 25)E_a}{298R(T_L + 273)}\right] \cdot \frac{\left[1 + \exp\left(\frac{298S - H}{298R}\right)\right]}{\left[1 + \exp\left(\frac{S(T_L + 273) - H}{R(T_L + 273)}\right)\right]} \quad (19)$$

where J_{max25} refers to J_{max} at 25 °C, E_a and R are as defined above, H is the curvature parameter determining the rate of J_{max} decrease above the peak temperature, and S is the entropy factor (Table 2).

Table 2 List of model parameters and their temperature dependencies (adopted from Yin and van Laar 2005)

	25 °C	E_a (kJ mol^{-1})	H (kJ mol^{-1})	S (kJ mol^{-1})
Parameters used for fitting				
K_C (μmol mol^{-1})	404.9	79.430		
K_O (mmol mol^{-1})	278.4	36.380		
Γ^* (μmol mol^{-1})	45.146	29.213		
Used for normalizing				
V_{cmax} (μmol m^{-2} s^{-1})	102.4	65.330		
J_{max} (μmol m^{-2} s^{-1})	160.0	37	219.4	704.2
T_P (μmol m^{-2} s^{-1})	11.55	53.1		
R_d (μmol m^{-2} s^{-1})	1.26	65.330		

2.5 Respiration

Adopting the method of ORYZA2000, respiration is modeled explicitly as the sum of maintenance and growth respiration (Bouman et al. 2001):

$$R_{sum} = R_m + R_g \quad (20)$$

where R_{sum} is total respiration, R_m the maintenance respiration at the temperature 25 °C, and R_g is the growth respiration.

$$R_{mr} = mc_{lv}\ W_{lv} + mc_{st}\ W_{st} + mc_{rt}\ W_{rt} + mc_{so}\ W_{so} \quad (21)$$

where R_{mr} is the maintenance respiration rate at the reference temperature (25 °C); W_{lv}, W_{st}, W_{rt}, and W_{so} are the weights of the leaves, stems, roots, and storage organs,

respectively; and mc_{lv}(0.02), mc_{st}(0.015), mc_{rt}(0.01), and mc_{so}(0.003) are the maintenance coefficients for leaves, stems, roots, and storage organs, respectively. The effect of temperature on maintenance respiration is simulated by:

$$R_m = T_{eff} R_{mr} \quad (22)$$

with

$$T_{eff} = 2^{(T_{av}-25)/10} \quad (23)$$

where T_{av} is the average daily temperature.

$$R_g = FSH(1.326FLV+1.326FST(1.-0.4) +1.11*0.4*FST+1.462*FSO)+1.326*FRT \quad (24)$$

where FSH is the fraction of total day matter allocated to shoots, FLV is the fraction of shoot day matter allocated to leaves, FST is the fraction of shoot day matter allocated to stems, FSO is the fraction of shoot day matter allocated to storage organs, and FRT is the fraction of total day matter allocated to roots.

2.6 Spatial integration and temporal integration

Adopting the concept of the two-leaf model (de Pury and Farquhar 1997; Wang and Leuning 1998), the canopy was divided into sunlit and shaded fractions and each fraction was modeled separately in a ' big-leaf' model. The radiation absorbed by the sunlit leaf fraction is calculated as an integral of the absorbed radiation and the sunlit leaf area fraction. The sunlit leaf area index of the whole canopy, L_{sun}, is given by:

$$L_{sun} = \frac{1-\exp(-k_b L_c)}{k_b} \quad (25)$$

where k_b is the beam radiation extinction coefficient (0.5/sin β where $\beta$is the solar elevation angle). The shaded leaf area index of the whole canopy, L_{sh} is

$$L_{sh} = L_c - L_{sun} \quad (26)$$

The radiation absorbed by the whole canopy is determined by integrating radiation absorbed over the entire canopy leaf area:

$$R_c = R_d(1-\rho_{cd})1-\exp(-k_d^{'}L_c) + R_b(1-\rho_{cb})[1-\exp(-k_b^{'}L_c)] \quad (27)$$

where R_b and R_d are incident direct-beam and diffuse radiation above the canopy, respectively; ρ_{cb} and ρ_{cd} are canopy reflection coefficients for direct-beam and diffuse radiation, respectively; k_b' and k_d' are the beam and scattered-beam radiation extinction coefficient (0.46/sin β), and the diffuse and scattered-diffuse radiation extinction coefficient (0.719), respectively.

The radiation absorbed by the sunlit fraction of the canopy, R_{sun} is given as the sum of direct-beam, diffuse, and scattered-beam components:

$$R_{sun} = R_b(1-\sigma)[1-\exp(-k_bL_c)] + R_d(1-\rho_{cd})k_d^{'}\frac{1-\exp(-k_d^{'}L_c-k_bL_c)}{k_d^{'}+k_b}$$
$$+ R_b\left\{(1-\rho_{cb})k_b^{'}\frac{1-\exp(-k_b^{'}L_c-k_bL_c)}{k_b^{'}+k_b} - (1-\sigma)\frac{1-\exp(-2k_bL_c)}{2}\right\} \quad (28)$$

where σ is the leaf scattering coefficient. Radiation absorbed by the shaded fraction of the canopy R_{sh} can be calculated as the difference between the R_c and R_{sun}:

$$R_{sh} = R_c - R_{sun} \quad (29)$$

Following Wang and Leuning (1998), the photosynthetic capacity of the sunlit-leaf fraction of the canopy, V_{csun}, and the shaded leaf fraction of the canopy, V_{csh}, can be calculated, respectively, by:

$$V_{csun} = V_{c\max}\frac{1-\exp(-k_nL_C+k_bL_c)}{k_n+k_b} \quad (30)$$

and

$$V_{csh} = V_{c\max}\left[\frac{1-\exp(-k_nL_c)}{k_n} - \frac{1-\exp(-k_nL_c-k_bL_c)}{k_n+k_b}\right] \quad (31)$$

where k_n is the coefficient of leaf nitrogen allocation, L_c is the canopy leaf area index,

and k_b is the extinction coefficient of beam irradiance.

The electron-transport capacity $J_{\max}$ over sunlit and shaded leaf fractions of the canopy are calculated as, respectively,

$$J_{msun} = J_{\max} \frac{1-\exp(-k_d L_C + k_b L_c)}{k_d + k_b} \tag{32}$$

and

$$V_{csh} = V_{c\max}[\frac{1-\exp(-k_d L_c)}{k_d} - \frac{1-\exp(-k_d L_c - k_b L_c)}{k_d + k_b}] \tag{33}$$

where k_d is the extinction coefficient for diffuse PAR (0.78).

The photosynthesis of the entire canopy is the sum of the photosynthesis fractions of sunlit and shaded leaves:

$$P_c = P_{sun} + R_{sh} \tag{34}$$

Following Goudriaan (1986), a numerical method is used for temporal integration. Daily canopy photosynthesis, P_c, is estimated by:

$$P_c = 0.0036 DYL \sum_{i=1}^{5} P_c(i) G_w(i) \tag{35}$$

where DYL is day length, $P_c(i)$ is instantaneous canopy photosynthesis at time $t(i)$, and $G_w(i)$ is the Gaussian weight at time $t(i)$.

3. COMPILING THE PROGRAM

The CERES-Rice model in DSSAT is a set of Fortran code and is usually complied with the Intel Fortran compiler (Intel Corporation, Santa Clara, CA, USA) on a Microsoft Windows operating system (Microsoft Corporation, Redman, Washington, USA). The detailed compiling procedures can be found in Thorp et al. (2012). A brief description

of using G95 under Eclipse in Windows 7 is given below.

The Java program (http://java.com/en/download/index.jsp) was installed in Windows 7. The Eclipse software (Juno Release, http://eclipse.org) was used to manage the compilations of the Fortran code. Photran (www.eclipse.org/photran) was the source code editor and debugging interface for Fortran programming in Eclipse. The open-source 'g95' compiler (http:// www.g95.org) built for use with MinGW (www.g95.org) was used to compile the code in this study. Photran utilizes makefile-based compilation, so we wrote a makefile to compile and build programs. The revised makefile is given in the Appendix.

4. TEST OF THE REVISED MODEL

4.1 Experimental data

The modified CERES-Rice model was tested against the datasets from rice experiments at four locations in Thailand and the Philippines collected in Singh et al. (1993). These experiments were chosen because they had been well-evaluated using the original CERES-Rice model.

The first experiment was called DTSP. The experimental site was in Thailand with six nitrogen treatments: 0, 38, 75, 113, 150, and 188 kg ha^{-1}. Fertilizers were applied two times on day 246 (3 September) and day 276 (3 October) of 1985, each time with half of the total fertilizer. The cultivar was RD 23. The location and soil properties are showed in Table 3. The planting date was day 246, 1985.

Table 3 The locations and soil properties of the four experiment sites used to test the CERES-Rice models

Name	DTSP	IRMZ	IPRI	IPRL
LAT	14.47	15.70	14.20	14.20
LONG	100.10	120.90	121.30	121.30
SLLL	0.245	0.258	0.28	0.289
SDUL	0.332	0.389	0.397	0.415
SSAT	0.398	0.65	0.412	0.7
SRGF	1	1	1	1
SBDM	1.41	0.85	1	0.75
SLOC	1.81	1.3	2.45	2.45
SLHW			6	6.2

LAT: Latitude, decimals. LONG: Longitude, decimals. SLLL: Lower limit, cm^3 cm^{-3}. SDUL: Drained upper limit, cm^3 cm^{-3}. SSAT: Upper limit, saturated, cm^3 cm^{-3}. SRGF: Root growth factor. SBDM: Bulk density, g cm^{-3}. SLOC: Organic carbon, %. SLHW: pH in water.

The mean weather data are shown in Table 4. Only October was wet with a total rainfall of 203.7 mm. The total monthly rainfall in December was only 0.5 mm.

Table 4 Mean weather data during the growth period for experiment DTSP in 1985

Mean	SEP	OCT	NOV	DEC
SRad	21.48	15.49	19.27	17.7
TMax	33	33.18	29.96	32.54
TMin	25.28	25.57	21.11	20.89
Rain	47	203.7	12.1	0.5
RNum	5	13	2	1

SRad: Daily solar radiation, MJ m^{-2} day^{-1}. TMax: Daily maximum temperature, ºC. TMin: Daily minimum temperature, ºC. Rain: Total rainfall, mm. RNum: Rainfall days, day.

The second experiment was called DRMZ. The experimental site was in the Philippines. The treatments were five nitrogen fertilizer levels, 0, 35, 70, 105, and 140 kg ha^{-1} combined with two irrigation treatments. Fertilizers were applied two times on day 54 (23 February) and day 77 (18 March) of 1986. The amount of fertilizer applied the first time was half of the amount of the second time. The cultivar was IR 58. The location and soil properties are shown in Table 3. The planting date was day 36 of 1986. The monthly mean weather data are listed in Table 5. The dry season lasted from February to April. There was no rainfall in March.

Table 5 Mean weather data during the growth period for experiment IRMZ in 1986

Mean	FEB	MAR	APR	MAY
SRad	16.76	20.9	23.97	19.35
TMax	31.61	34.01	35.15	37.67
TMin	20.93	22.39	23.77	26.76
Rain	46	0	25	269.1
RNum	6	0	3	22

See table 4 for definitions of abbreviations.

The third experiment was named IPRI. The experimental site was located in the Philippines. The tested data were selected from eight treatments of four nitrogen fertilizer levels, 0, 30, 60, and 120 kg ha^{-1}, combined with two irrigation treatments. Fertilizers were applied one time on day 8 (8 January) of 1980. The cultivar was IR 36. The location and soil properties are shown in Table 3. The planting date was day 9 of 1980. The monthly mean weather data are listed in Table 6. The dry season was in January and February.

Table 6 Mean weather data during the growth period for experiment IRPI in 1980

Mean	JAN	FEB	MAR	APR
SRad	14.34	17.78	18.4	20.76
TMax	29.62	30.96	32.08	32.79
TMin	21.39	20.86	21.22	23.36
Rain	17.5	15.83	122.3	99.4
RNum	9	6.76	8	6

See table 4 for definitions of abbreviations.

The fourth experiment was named IPPL. The experimental site was located in the Philippines. The ten treatments were five nitrogen fertilizer levels, 0, 30, 60, and 120 kg ha^{-1}, combined with two irrigation treatments. Fertilizers were applied two times on day 53 (22 February) and day 73 (14 March) of 1985. The cultivar was IR 58. The location and soil properties are shown in Table 3. The planting date was day 35 of 1985. The monthly mean weather data are listed in Table 7. The whole growth period was dry.

Table 7 Mean weather data during the growth period for experiment IRPI in 1980

Mean	FEB	MAR	APR	MAY
SRad	18.74	19.03	18.51	20.05
TMax	29.96	30.15	32.08	32.11
TMin	22.56	22.64	23.37	23.96
Rain	11.6	26.8	37.2	53.7
RNum	7	15	7	8

See table 4 for definitions of abbreviations.

4.2 Future climate data

The future data were generated using the web-based software tool MarkSim™ DSSAT weather file generator (http://gismap.ciat.cgiar.org/MarkSimGCM) (Jones and Thornton 2013). We assumed that the CO_2 concentration will be 400 ppm in 2020, 550 ppm in 2050, and 750 ppm in 2090. The general circulation model (GCM) was ECHam5 with climate scenarios A1b, A2, and B1. MarkSim™ used a generalized downscaling and data generation method, which takes the outputs of a GCM describing a particular future climate and allows the stochastic generation of a core set of daily weather data that are somewhat characteristic of this future climate. Figures 4A and B show the variation of the maximum and minimum temperature from day 1 to day 160. Compared with 1986, the average maximum temperature increased by 2.1, 2.98, and 4.89 °C in 2020, 2050, and 2090, respectively; and the average minimum temperature increased by 0.20, 1.28, and 2.82 °C, in 2020, 2050, and 2090, respectively. The maximum temperature increased much fast than minimum temperature.

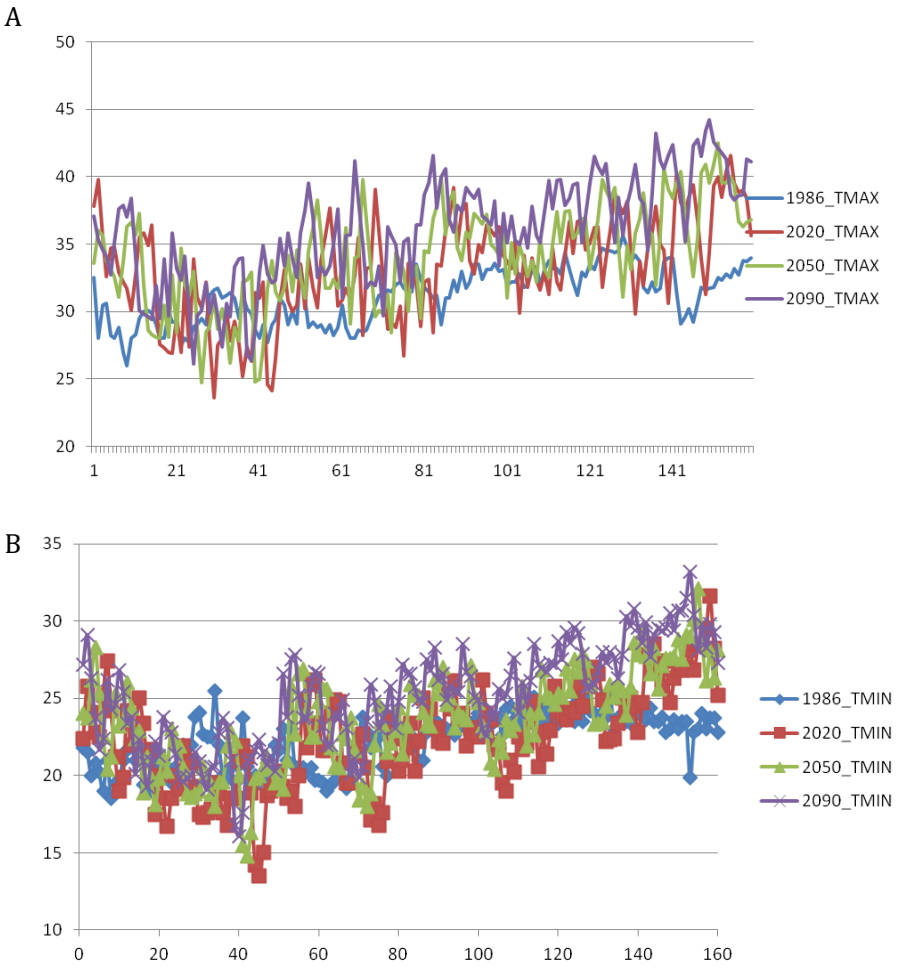

Figure 4 Comparison of the variation of max temperature (A) and minimum temperature (B) in 1986, 2020, 2050, and 2090. Data in 1986 were from observations. Data in other years were generated using the MarkSim™ DSSAT weather file generator.

5. RESEARCH RESULTS

5.1 Rice yield and growth under current environmental conditions

1) Ricce yield

Yield data were available at harvest for all four sites. The simulated yields using both models of the treatment with 0 N were slightly lower than the observed yield. The simulated yield using the revised model with 38 kg ha^{-1} N application was very close to the observed yield. However, the simulated yields using both models were greater than the observed yield when the applied N was more than 38 kg ha^{-1}. The regression equation for yield simulated using the original model was y = 1.753x - 2311 with r^2 = 0.975 and an RMSE (Root Mean Square Error) of 913 kg ha^{-1}. The regression equation for yield simulated using the revised model was y = 1.64 + 2028 with r^2 = 0.968 and an RMSE of 753 kg ha^{-1} (Fig. 5). The closer results between the simulated and observed yields indicated that the revised model was better than the original model.

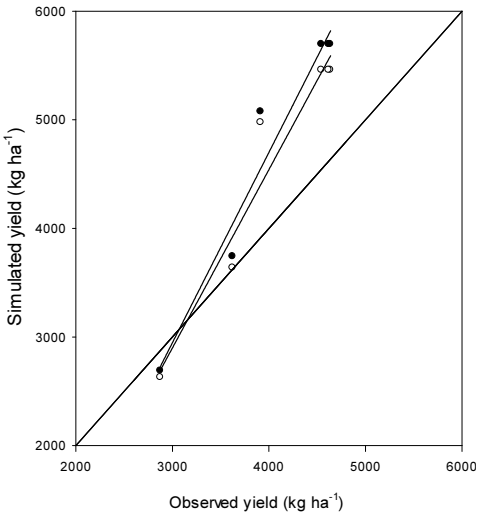

Figure 5 Simulated and observed rice grain yields at the six nitrogen treatments of experiment DTSP. Black circles indicate yields simulated using the original CERES-Rice model, while open circles indicate yields using the revised model.

The simulated yields in experiment IRMZ using both models are shown in Figure 6. The treatments were two irrigation levels combined with 5 nitrogen application levels. The impact of the irrigation treatments on the simulated yield was not significant. The yields were different from those in the experiments in DTSP, increasing with higher N application levels up to 140 kg N. The simulated yields were slightly lower than the observed values when less N was applied but slightly overestimated at higher N application levels. The regression for yields from the original model was $y = 1.328x - 1367$ with $r^2 = 0.991$ and an RMSE of 756 kg ha^{-1}. The regression equation for the yield using the revised model was $y = 1.263x - 1196$ with $r^2 = 0.991$ and an RMSE of 572 kg ha^{-1}. The simulated yields in IRMZ using the revised model were closer to the observed yield.

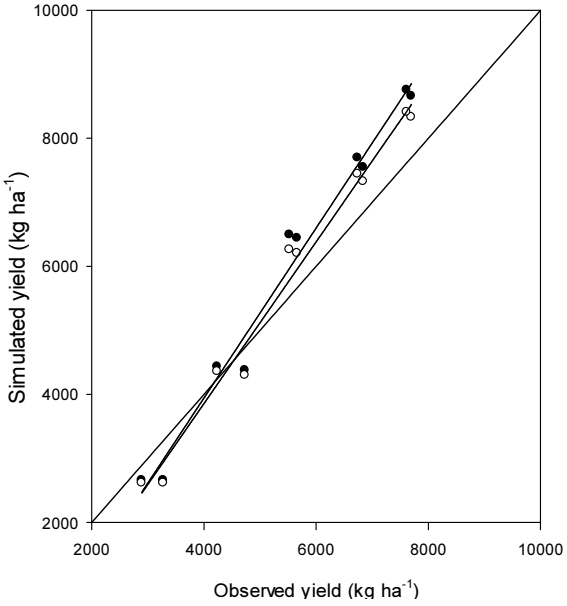

Figure 6 Simulated and observed rice grain yields at the six nitrogen treatments of experiment IRMZ. Black circles denote yields simulated using the original CERES-Rice model, while open circles denote yields using the revised model.

The IRPI experiment had nine treatments: three N application levels combined with three irrigation levels. The differences between simulated yields using both models were small when N application levels were low, but the differences were large at higher levels. This may imply that the N cycle in the model influenced the

nitrogen contents in leaves, which determined the photosynthetic capacity. The regression for the original model yields was y = 0.906x + 0.806 with r^2 = 0.682 and an RMSE of 646 kg ha^{-1}. The regression equation for the yield using the revised model was y = 0.839x + 996 with r^2 = 0.671 and an RMSE of 579 kg ha^{-1}. The simulated yields using the revised model were closer to the observed yield with low N application levels. However, at higher levels, yields simulated using the revised model were very close to observed values (Fig. 7).

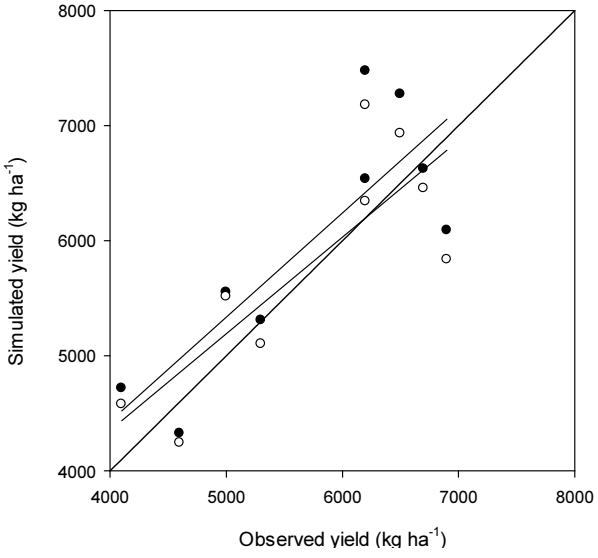

Figure 7 Simulated and observed rice grain yields at the six nitrogen treatment levels of IRPI. Black circles denote yields simulated using the original CERES-Rice model, open circles denote yields using the revised model.

Experiment IPPL had ten treatments: five N application levels combined with two irrigation levels. The simulated yields using both models were closer (Fig. 8). Except for the 0 and 60 kg N treatments, the simulated yields using both models were slightly more than the observed yields. The regression for the original model yields was y = 1.33x - 1276 with r^2 = 0.951 and an RMSE of 659 kg ha^{-1}. The regression equation for the yield using the revised model was y = 1.24x + 1000 with r^2 = 0.951 and an RMSE of 506 kg ha^{-1}. The simulated yields using the revised model were closer to observed yields.

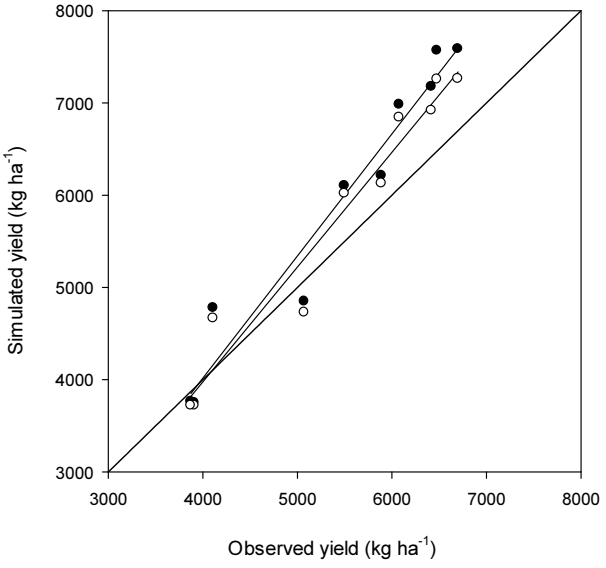

Figure 8 Simulated and observed rice grain yields at the six nitrogen treatment levels of experiment IRPL. Black circles denote yields simulated using the original CERES-Rice model, while open circles denote yields using the revised model.

2) Rice tops biomass

Aboveground biomass included leaf, stem, and ear masses. Since there were no root biomass observations available, we could not evaluate the model using total biomass. Figure 9 shows the relationships between simulated tops weights using both models and the observed tops weights. For the treatments with no N application, the simulated weights using both models were almost the same and the values were small. In the high N treatments, the simulated tops weights using the revised model were closer to the observed values than the values simulated using the original model. The regression equation for the original model for tops weights was y = 1.27x - 1603 with r^2 = 0.887 and an RMSE of 1449 kg ha^{-1}. The regression equation for the tops weights using the revised model was y = 1.16x - 928 with r^2 = 0.868 and an RMSE of 890 kg ha^{-1}. The simulated yields from the revised model were closer to the observed values than to those from the original model.

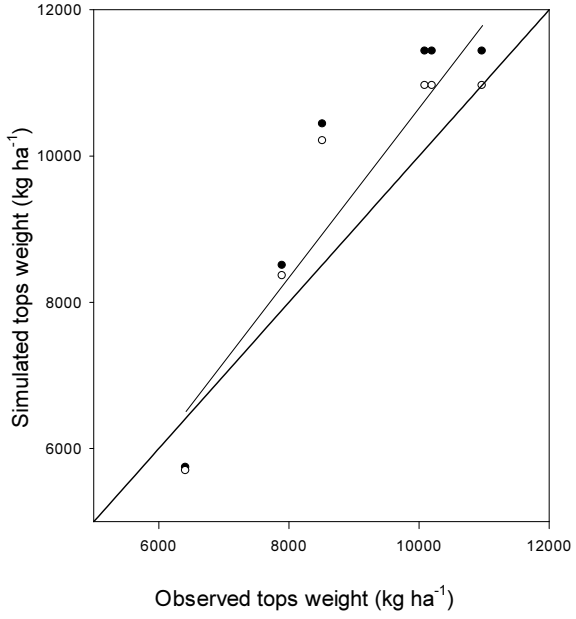

Figure 9 Simulated and observed rice tops weights at the six nitrogen treatment levels of experiment DTSP. Black circles denote values simulated using the original CERES-Rice model, while open circles denote values using the revised model.

Simulated and observed tops weights of experiment IRMZ are shown in Figure 10. The simulated weights using both models were similar to the observed values when there was no N application. With increasing N application, the simulated values became larger than the corresponding observed values. The regression equation for the original model for tops weights was y = 1.415x - 1419 with r^2 = 0.960 and an RMSE of 2433 kg ha^{-1}. The regression equation for the tops weights using the revised model was y = 1.38x - 1399 with r^2 = 0.961 and an RMSE of 2125 kg ha^{-1}. The simulated values using the revised model were closer to the observed values than those from the original model.

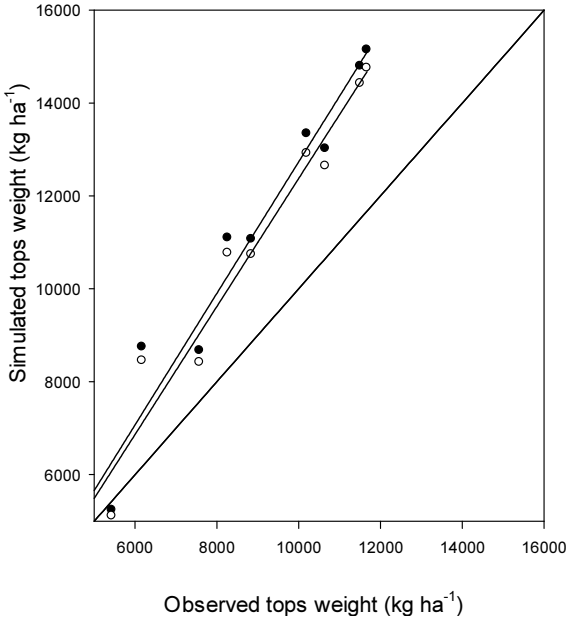

Figure 10 Simulated and observed rice tops weights at the six nitrogen treatment levels of experiment IRMZ. Black circles denote weights simulated using the original CERES-Rice model, while open circles denote those from the revised model.

The trends of the simulated tops weights for experiment IRPI using both models were similar to the observed tops weights but with a low intercept (Fig. 11). With a large N application, the simulated weight were very different from observed values. The regression equation for the original model tops weights was y = 1.20x - 701 with r^2 = 0.728 and an RMSE of 1892 kg ha^{-1}. The regression equation for the tops weights using the revised model was y = 1.14x - 523 with r^2 = 0.728 and an RMSE of 1468 kg ha^{-1}. The simulated yields using the revised model were closer to observed values than those from the original model.

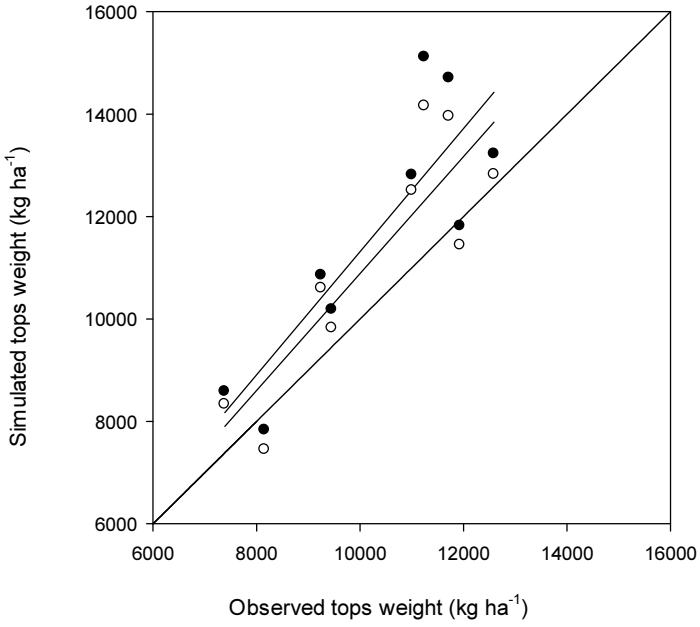

Figure 11 Simulated and observed rice tops weights at the six nitrogen treatment levels of experiment IRPI. Black circles denote values simulated using the original CERES-Rice model, while open circles denote those from the revised model.

The trends of the simulated tops weights of IRPL using both models were similar to the observed tops weights but with an intercept (Fig. 12). The difference between the simulated values of the models was similar in different treatments. The regression equation for the original model for tops weights was y = 1.27x - 600 with r^2 = 0.963 and an RMSE of 2877 kg ha^{-1}. The regression equation for the tops weights using the revised model was y = 1.19x - 912 with r^2 =0.958 and an RMSE of 2578 kg ha^{-1}. The simulated yields using the revised model were closer to the observed values than those from the original model.

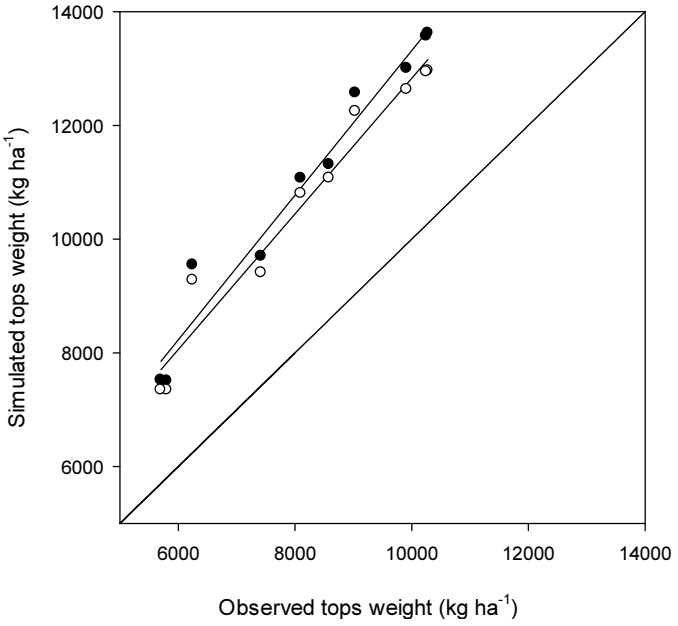

Figure 12 Simulated and observed rice tops weights at the six nitrogen treatment levels of experiment IRPL. Black circles denote values simulated using the original CERES-Rice model, while open circles denote those from the revised model.

5.2 Rice yield and growth under future climate and CO_2 conditions

Since we mainly focused on the comparison between original and revised models and there were no experimental data available under future climate and enrichment CO_2 conditions, in this section, we assumed that the rice cultivars, soil conditions, and management practices would not change in the future for all experimental sites. We simulated rice growth and yield in DTSP and IRMZ using both models.

1) Rice yield

The impact of climate change on rice yield depended on the scenarios. Figure 13 shows simulated results using both models for experiment DTSP. When comparing the observed yields with all treatments in 1985, the simulated yields were much lower under scenario A2. In 2020, simulated yields were zero except in the 0 N

treatment. Surprisingly, in 2090, under scenarios A1b and B1, the simulated yields from every treatment (except the 0 N treatment) using both models were greater than the observed yields in 1985. In 2050, under scenarios A2 and B1, simulated yields with higher N application could be higher than the observed yields in 1985. However, the simulated yields in 2050 with all treatments were less than the observed yields in 1985. The simulated yields using the revised model were less than the yields simulated using the original model, and the magnitude depended on the treatment.

The simulated yields of experiment IPMZ showed similar trends with different N application levels under different scenarios (Fig. 14). In the two low N treatments, the simulated yields were less than the observed yields under all climate scenarios. For all other cases, the simulated yields using both models could be higher or lower than the observed yields.

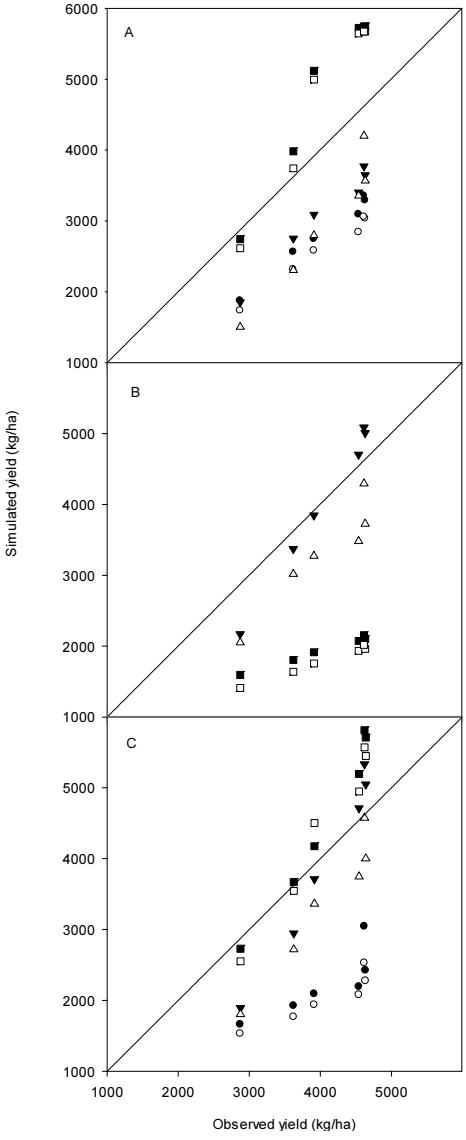

Figure 13 Comparison of observed and simulated yields of experiment DTSP under future climate and CO_2 concentrations using both models. Black symbols denote the results using the original model and open symbols denote the results using the revised model. The simulated yields under scenarios A1b, A2, and B1 are in A, B, and C, respectively. Circles, triangles, and squares represent results in 2020, 2050, and 2090, respectively.

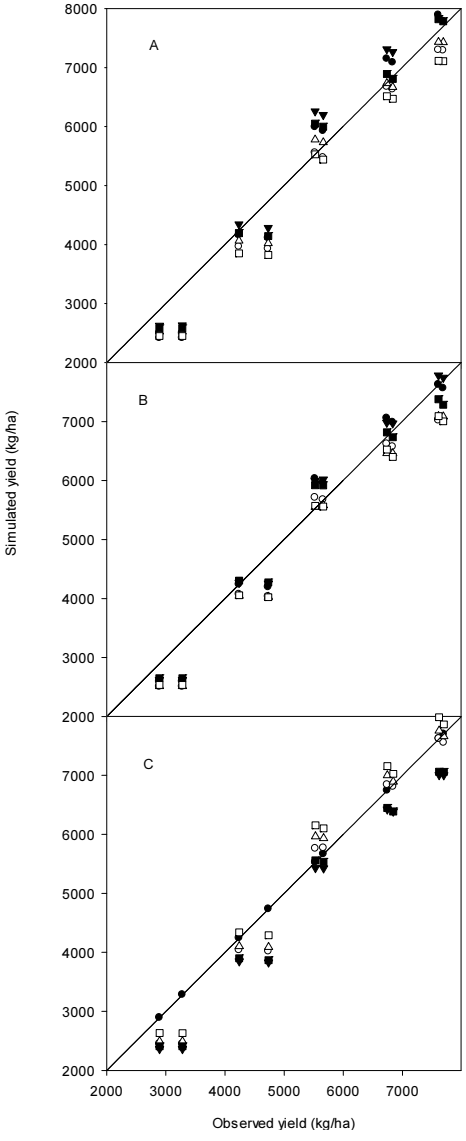

Figure 14 Comparison of observed yields and simulated yields of experiment IPMZ under future climate and CO_2 concentrations using both models. Black symbols denote the results using the original model and open symbols denote the results using the revised model. The simulated yields under scenarios A1b, A2, and B1 are in A, B, and C, respectively. Circles, triangles, and squares represent results in 2020, 2050, and 2090, respectively.

2) Rice growth

The differences in simulated rice aboveground biomass in experiment DTSP in different years were dependent on the climate scenarios and treatments (Fig. 15). Generally, the lowest tops weights were simulated for 2020. The highest values under scenarios A1b and B1 were in 2090, and under scenario A2 were in 2050, suggesting that the impacts of climate change on rice growth depended on the climate scenario. The final yield changes relied on the interaction among the climate, CO_2 concentration, and treatment.

The simulated rice tops weights of experiment IRMZ using both models were larger than the observed values in 1986. The differences between simulated and observed values were larger with increasing N application. The simulated values in 2050 were the largest for the different treatments (Fig. 14).

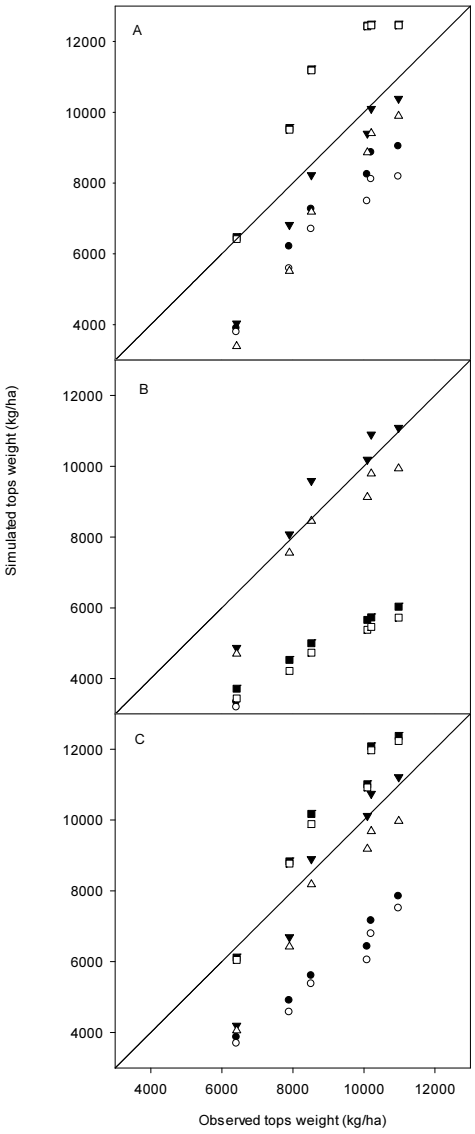

Figure 15 Comparison of observed and simulated tops weights of experiment DTSP under future climate and CO_2 concentrations using both models. Black symbols denote the results using the original model and open symbols denote the results using the revised model. The simulated tops weights under scenarios A1b, A2, and B1 are in A, B, and C, respectively. Circles, triangles, and squares represent results in 2020, 2050, and 2090, respectively.

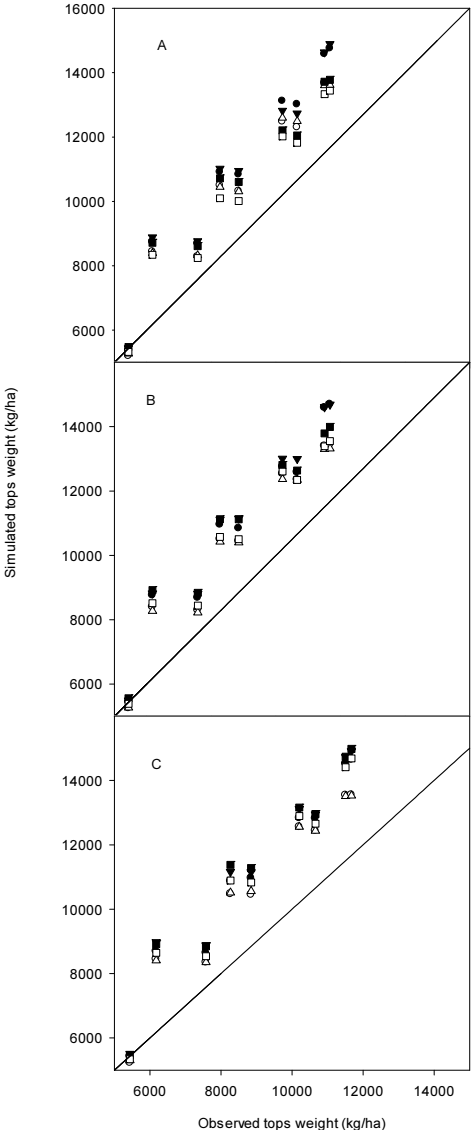

Figure 16 Comparison of observed and simulated tops weights of experiment IPMZ under future climate and CO_2 concentrations using both models. Black symbols denote the results using the original model and open symbols denote the results using the revised model. The simulated tops weights under scenarios A1b, A2, and B1 are in A, B, and C, respectively. Circles, triangles, and squares represent results in 2020, 2050, and 2090, respectively.

5.3 Application of the CERES-Rice model

The model can be used for improving rice management. As an example, we only tested the application for changes in transplanting date using the revised CERES-Rice model. Assuming only changes in climate and CO_2 concentration in 2090, we simulated rice yields with different transplanting dates from 29 January to 10 February 2090 under climate scenario A1B. Figure 17 shows the simulated yields with different treatments. They varied greatly with different transplanting dates, suggesting that this factor is very important for optimizing rice yield. The date in red indicates the maximum yield for a certain treatment; for example, for treatment 5, the best transplanting date would be 1 February, five days earlier than it was in 1986.

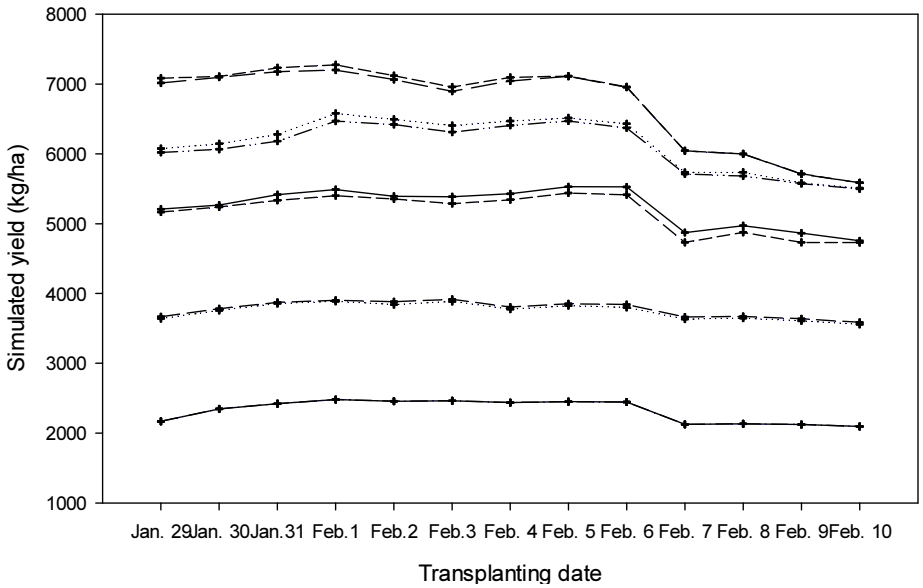

Figure 17 The simulated yields of experiment IPMZ using the revised CERES-Rice model under scenario A1B in 2090 with different transplant dates. Each line is for a different N treatment.

6. CONCLUDING REMARKS

We revised the CERES-Rice model by replacing the radiation use efficiency equation for rice growth in the original CERES-Rice model with the biochemical FvCB model for the photosynthetic rate. This model can be used to simulate the impacts of climate change and CO_2 enrichment on rice growth and yield, and to evaluate the interactions between rice plants and the environment. The simulated results from the revised model were more similar than the original to observed data on rice growth and yield for the three cultivars from four experiments on N application and irrigation conducted in Thailand and the Philippines. The simulated rice yield increased or decreased depending on the climate scenario. This study illustrated the potential for the application of the revised model to determine optimal management practices, such as the transplanting date, under different environmental conditions. However, further evaluation of the revised model is needed under changing climate conditions, such as using the data from FACE experiments. Based on the results from this study, it can be reported that the revised CERES-Rice model performs better than the original and can be used for forecasting rice yields and determining optimal management practices.

REFERENCES

Boote, K. J., and N. B. Pickering, 1994: Modeling photosynthesis of row crop canopies. *HortScience*, **29,** 1423-1434.

Bouman, B. A. M., M. J. Kropff, T. P. Tuong, M. C. S. Wopereis, H. F. M. ten Berge, and H. H. Van Laar, 2001: *ORYZA2000: Modeling Lowland Rice*. International Rice Research Institute, 235 pp.

Challinor, A. J., T. R. Wheeler, P. Q. Craufurd, J. M. Slingo, and D. I. F. Grimes, 2004: Design and optimisation of a large-area process-based model for annual crops. *Agric. For. Meteorol.*, **124,** 99-120.

Cho, J., and T. Oki, 2012: Application of temperature, water stress, CO2 in rice growth models. *Rice*, **5** (1), 1-8.

de Pury, D. G. G., and G. D. Farquhar, 1997: Simple scaling of photosynthesis from leaves to canopy without the errors of bigleaf models. *Plant Cell Environ.,* **20,** 537-557.

Farquhar, G. D., S. von Caemmerer, and J. A. Berry, 1980: A biochemical model of photosynthetic CO2 assimilation in leaves of C3 species. *Planta*, **149,** 78-90.

Farquhar, G. D., and S. C. Wong, 1984: An empirical model of stomatal conductance. *Aust. J. Plant Physiol.*, **11,** 191-210.

Goudriaan, J., 1977: *Crop Micrometeorology: A Simulation Study.* PUDOC.

Goudriaan, J., 1986: A simple and fast numerical method for the computation of daily totals of crop photosynthesis. *Agric. For. Meteorol.*, **38,** 249-254.

Harley, P. C., F. Loreto, G. di Marco, and T. D. Sharkey, 1992a: Theoretical consideration when estimating the mesophyll conductance to CO2 flux by analysis of the response of photosynthesis to CO2. *Plant Physiol.*, **98,** 1429-1436.

Harley, P. C., R. B. Thomas, J. F. Reynolds, and B. R. Strain, 1992b: Modelling photosynthesis of cotton grown in elevated CO2. *Plant, Cell Environ.*, **15,** 271-282.

Horie, T., H. Nakagawa, H. G. S. Centeno, and J. M. Kropff, 1995: The rice crop simulation model SIMRIW and its testing. *Modelling the Impact of Climate Change on Rice Production in Asia*, R. B. Matthews, M. J. Kropff, and D. Bachelet, Eds., CAB International, 51-66.

Howden, S. M., J. F. Soussana, F. N. Tubiello, N. Chhetri, M. Dunlop, and H. Meinke, 2007: Adapting agriculture to climate change. *Proc. Natl. Acad. Sci. U. S. A.*, **104,** 19691-19696.

Hunt, L. A., and K. J. Boote, 1994: Data for model operation, calibration, and validation.

IBSNAT: A System Approach to Research and Decision Making, G. Y. Tsuji, G. Hoogenboom, and P. K. Thornton, eds., University of Hawaii, 9-40.

IPCC, 2007: *Contribution of Working Group I to the Fourth Assessment Report of the Intergovernmental Panel on Climate Change*, Cambridge University Press.

Jiang, M., and Z. Jin, 2009: A method for up scaling genetic parameters of CERES-Rice in regional applications. *Rice Sci.*, **16,** 292-300.

Jones, J. W., G. Hoogenboom, C. H. Porter, K. J. Boote, W. D. Batchelor, L. A. Hunt, P. W. Wilkens, U. Singh, A. J. Gijsman, and J. T. Ritchie, 2003: The DSSAT cropping system model. *Eur. J. Agron.*, **18** (3), 235-265.

Jones, P. G., and P. K. Thornton, 2013: Generating downscaled weather data from a suite of climate models for agricultural modelling applications. *Agric. Syst.*, **114,** 1-5.

Kim, J., S. Han, H. Kim, and Y. Kim, 2002: Using spatial data and crop growth modeling to predict performance of South Korean rice varieties grown in western coastal plains in North Korea. *Korean. J. Agric. For. Meteorol.*, **4** (4), 224-236.

Lee, T., J. Choi, S. Yoo, S. Lee, and Y. Oh, 2012: Analyzing consumptive use of water and yields of paddy rice by climate change. *J. Korean Soc. Agric. Eng.*, **54** (1), 47-54.

Lobell, D. B., W. Schlenker, and J. Costa-Roberts, 2011: Climate trends and global crop production since 1980. *Science*, **333,** 616-620.

Medlyn, B. E., E. Dreyer, D. Ellsworth, M. Forstreuter, P. C. Harley, M. U. F. Kirschbaum, X. Le Roux, P. Montpied, J. Strassemeyer, A. Walcrofe, K. Wang, and D. Loustau, 2002: Temperature response of parameters of a biochemically based model of photosynthesis. II. A review of experimental data. *Plant, Cell Environ.*, **25,** 1167-1179.

Meinshausen, M., S. J. Smith, K. V. Calvin, J. S. Daniel, M. L. T. Kainuma, J. F. Lamarque, K. Matsumoto, S. A. Montzka, S. C. B. Raper, K. Riahi, A. M. Thomson, G. J. M. Velders, and D. van Vuuren, 2011: The RCP greenhouse gas concentrations and their extension from 1765 to 2300. *Clim. Change*, **109** (1-2), 213-241.

Monsi, M., and T. Saeki, 1953. Über den lichtfaktor in den pflanzengesellschaften und seine bedeutung fur die stoffproduktion. *Jpn. J. Bot.*, **14,** 22-52.

Morison, J. I. I., 1987: Intercellular CO2 concentration and stomatal response to CO2. *Stomatal Function*, E. Zeiger, G. D. Farquhar, and I. R. Cowan, Eds., Stanford Univ. Press., 1-15.

Rosenzweig, C., J. W. Jones, J. L. Hatfield, A. C. Ruane, K. J. Boote, P. J. Thorburn, J. M. Antle, G. C. Nelson, C. H. Porter, S. Janssen, S. Asseng, B. Basso, F. Ewert, D. Wallach, G. A. Baigorria, and J. M. Winter, 2013: The Agricultural Model Intercomparison and Improvement Project (AgMIP): Protocols and pilot studies. *Agric. For. Meteorol.*, **170,** 166-182.

Rotter, R. P., T. R. Carter, J. E. Olesen, and J. R. Porter, 2011: Crop-climate models need an overhaul. *Nat. Clim. Change*, **1,** 175-177.

Sarkar, R., and S. Kar, 2008: Sequence analysis of DSSAT to select optimum strategy of crop residue and nitrogen for sustainable rice-wheat rotation. *Agron. J.* **100,** 86-97.

Sharkey, T. D., C. J. Bernacchi, G. D. Farquhar, and E. L. Singsaas, 2007: Fitting photosynthetic carbon dioxide response curves for C3 leaves. *Plant, Cell Environ.*, **30,** 1035-1040.

Singh, U., J. T. Ritchie, and D. C. Godwin, 1993: *A Users Guide to CERES-rice V2.10. Simulation Manual IFDC-SM-4*, IFDC, 131 pp.

Singh, U., J. Timsina, and D. C. Godwin, 2002: Testing and applications of CERES-rice and CERES-wheat models to rice-wheat cropping systems. *Modelling Irrigated Cropping Systems, with Special Attention to Rice-Wheat Sequences and Raised Bed Planting.* Proceedings. *Workshop at CSIRO Land and Water, Griffith (Australia) 25-28 February 2002*, E. Humphreys, and J. Timsina, Eds., 17-32.

Thorp, K. R., J. W. White, C. H. Porter, G. Hoogenboom, G. S. Nearing, and A. N. French, 2012: Methodology to evaluate the performance of simulation models for alternative compiler and operating system

configurations. *Comput. Electron. Agric.* **81,** 62-71.

Timsina, J., and E. Humphreys, 2006: Performance of CERES-Rice and CERES-Wheat models in rice-wheat system: a review. *Agric. Syst.* **90,** 5-31.

Wang, Y. P., and R. Leuning, 1998: A two-leaf model for canopy conductance, photosynthesis and portioning of available energy I: Model description and comparison with a multi-layered model. *Agric. For. Meteor.*, **91,** 89-111.

Wullschleger, S. T., 1993: Biochemical limitations to carbon assimilation in C3 plants - a retrospective analysis of the A-Ci curves from 109 species. *J. Exp. Bot.*, **44,** 907-920.

Yang, W., H. S. Cho, M. Kim, K. Y. Seong, T. S. Park, M. C. Seo, and H. W. Kang, 2013: Re-examination of the standard cultivation practices of rice in response to climate change in Korea. *J. Crop Sci. Biotechnol.*, **169** (2), 85-92.

Yin, X., and H. H. Van Laar, 2005: *Crop Systems Dynamics: An Ecophysiological Simulation Model for Genotype-by-Environment Interactions*, Wageningen Academic Publishers.

APCC RESEARCH REPORT 2013-07

- Predicting Potential Epidemics of Rice Leaf Blast and Sheath Blight in South Korea under the RCP 4.5 and RCP 8.5 Climate Change Scenarios using a Rice Disease Epidemiology Model, EPIRICE
- Prediction of the Seasonal Tropical Cyclone Activity in the Western North Pacific using an APCC MME-Based Statistical Approach
- Simple Statistical Bias Correction for Climate Change Applications
- Revising the DSSAT/CERES-Rice Model to Simulate the Impacts of Climate Change on Rice Yield in Asia
- Development of a Regional Rice Model for Assessing the Impact of Climate Change on Rice in South Korea

APEC Climate Center

12, Centum 7-ro, Haeundae-gu, Busan 612-020,
Republic of Korea
Tel: +82-51-745-3900 Fax: +82-51-745-3949
www.apcc21.org

비매품
94550
9 788997 333998
ISBN 978-89-97333-99-8
ISBN 978-89-97333-92-9 (세트)